

The Recent and Submerged Tombolos—Unique Phenomena on the Adriatic Sea

Benac, Čedomir; Bočić, Neven; Wacha, Lara; Maglić, Lovro; Ružić, Igor

Source / Izvornik: **Journal of Marine Science and Engineering, 2024, 12**

Journal article, Published version

Rad u časopisu, Objavljena verzija rada (izdavačev PDF)

<https://doi.org/10.3390/jmse12091575>

Permanent link / Trajna poveznica: <https://urn.nsk.hr/urn:nbn:hr:157:127696>

Rights / Prava: [Attribution 4.0 International](#)/[Imenovanje 4.0 međunarodna](#)

Download date / Datum preuzimanja: **2025-04-02**



Repository / Repozitorij:

[Repository of the University of Rijeka, Faculty of Civil Engineering - FCERI Repository](#)



Article

The Recent and Submerged Tombolos—Unique Phenomena on the Adriatic Sea

Čedomir Benac ¹, Neven Bočić ^{2,*}, Lara Wacha ³, Lovro Maglić ⁴ and Igor Ružić ⁵

¹ Faculty of Civil Engineering, University of Rijeka, R. Matejčić 3, 51000 Rijeka, Croatia; cbenac@uniri.hr

² Department of Geography, Faculty of Science, University of Zagreb, Trg M. Marulića 19, 10000 Zagreb, Croatia

³ Department of Geology, Croatian Geological Survey, M. Sachsa 2, 10000 Zagreb, Croatia; lwacha@hgi-cgs.hr

⁴ Department of Nautical Sciences, Faculty of Maritime Studies, University of Rijeka, Studentska 2, 51000 Rijeka, Croatia; lovro.maglic@pfri.uniri.hr

⁵ Department for Hydrotechnics and Geotechnics, Faculty of Civil Engineering, University of Rijeka, R. Matejčić 3, 51000 Rijeka, Croatia; iruzic@gradri.uniri.hr

* Correspondence: nbocic@geog.pmf.hr

Abstract: Prvić Island (Kvarner area in the NE channel part of the Adriatic Sea) is a part of the Natura 2000 protected area network. A recent tombolo is located on the SW coast of Prvić Island, and much larger submerged tombolos are located on the shoal towards the south. Both phenomena are unique to the Croatian coast of the Adriatic Sea. The inland part of the tombolo was surveyed using an Unmanned Aerial Vehicle, and a 3D point cloud was created using Structure from Motion with Multi-View Stereo photogrammetry. The body of the talus breccia behind the tombolo has a triangular form. Large collapsed rocky blocks form the cape vertex. This cape is in a state of equilibrium in the present oceanographic conditions but might be eroded due to predicted rises in sea level. The submarine zone was explored using scuba-diving equipment and Remotely Operated Vehicles. A large triangle-shaped shoal consists of flysch. Parallel vertical sandstone layers that look like artificially built walls are more than a hundred metres long. The carbonate breccia is located at the end of the shallow zone. The conditions for the final formation of the submerged shoal were created during the sea level stagnation in the Holocene.

Keywords: tombolo; marine erosion; slope instability; flysch; sea level; climate change



Citation: Benac, Č.; Bočić, N.; Wacha, L.; Maglić, L.; Ružić, I. The Recent and Submerged Tombolos—Unique Phenomena on the Adriatic Sea. *J. Mar. Sci. Eng.* **2024**, *12*, 1575. <https://doi.org/10.3390/jmse12091575>

Academic Editor: Kyu-Han Kim

Received: 24 July 2024

Revised: 21 August 2024

Accepted: 30 August 2024

Published: 6 September 2024



Copyright: © 2024 by the authors. Licensee MDPI, Basel, Switzerland. This article is an open access article distributed under the terms and conditions of the Creative Commons Attribution (CC BY) license (<https://creativecommons.org/licenses/by/4.0/>).

1. Introduction

A tombolo is a depositional geomorphological landform (sandbar, barrier, or spit) that joins an island or a barrier with either the mainland or another island, resulting from longshore drift or the migration of an offshore bar toward the coast [1]. Tombolos' lengths vary from a few tens of metres behind small obstacles, up to more than ten kilometres. Single tombolos are the most common, but there are also tombolo pairs and triplets [2–4]. Three geomorphological factors are important for the preconditions for tombolo formation: (i) high sediment supply, (ii) a physical barrier against the swell, and (iii) coastal processes conducive to the development of a sandbank, i.e., bidirectional currents converging towards this physical barrier ([5] according to [2]).

Although they are a relatively rare geomorphological phenomenon, they have been studied all over the world, e.g., Finland [6], Australia [7], Japan [8], and Great Britain [9,10]. There are also several tombolos in the Mediterranean Sea, e.g., Italy [3,11], France [12,13], Lebanon [2,14], Turkey [4], and Egypt [15].

A coastal and submerged karst relief prevails on the Croatian part of the Adriatic Sea [16]. The Kvarner area is a part of the northwestern Adriatic channel zone where karstified carbonate rock predominates, while flysch rocks occur sporadically [17]. The present relief is a consequence of sea level changes and recent tectonic movements [18].

The submerged karst relief is visible in many places, while outcrops of flysch are mostly covered by younger sediments and are therefore rarely visible on the sea floor [19].

The recent tombolo and the much bigger submerged tombolo are located on the southwestern coast of Prvić Island in the Kvarner area (Figure 1). However, their lithologic composition and tectonic fabric, morphogenesis, and present and future geomorphological processes are not well understood. [20].

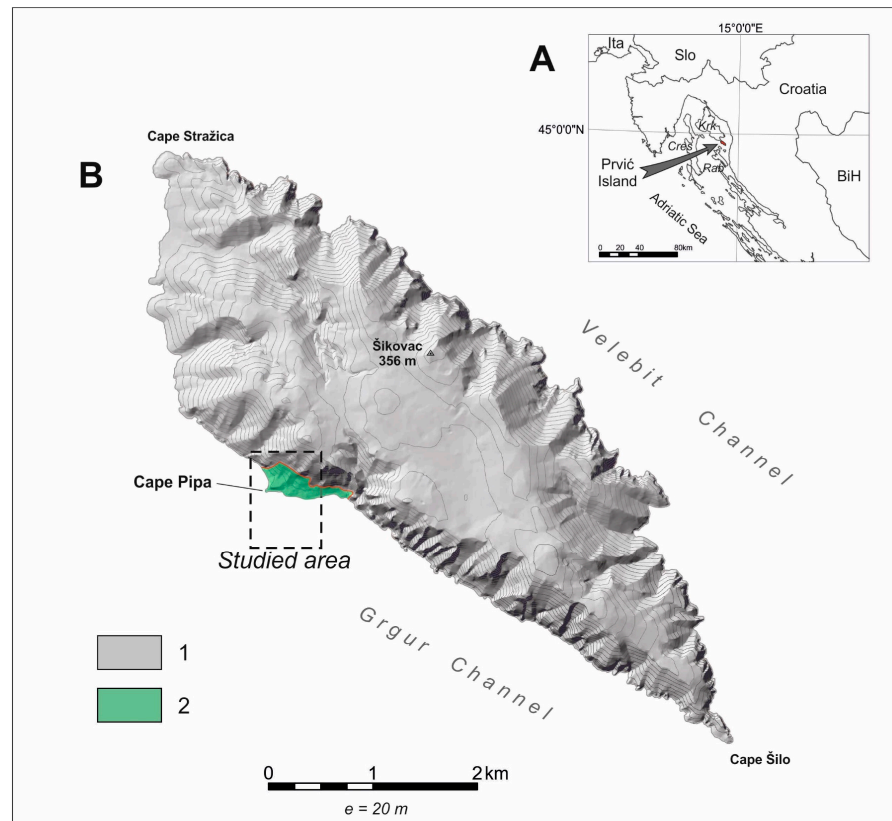


Figure 1. (A)—The position of Prvić Island in the Kvarner area; (B)—simplified geological map: 1—carbonate rocks, 2—flysch (the background is a hill shade based on the 5×5 m DEM).

These geomorphological phenomena co-existing nearby are a unique phenomenon in the Adriatic Sea, and possibly in the Mediterranean Sea, so knowing their characteristics is very important. This especially applies to their conservation, because the wide area of Prvić Island is under the protection of the Natura 2000 network [21].

In addition to standard geological and geomorphological methods, detailed survey methods were also used. The inland part was surveyed using an Unmanned Aerial Vehicle (UAV), and a 3D point cloud was generated using Structure from Motion (SfM) with Multi-View Stereo (MVS) photogrammetry. The submerged zone was surveyed using scuba-diving equipment and Remotely Operated Vehicles (ROVs).

The research presented in this paper aims to clarify the conditions and processes of the morphogenesis of these two tombolos, to establish present geomorphological processes with the main purpose of their better preservation and quality interpretation, and to create a realistic scenario of the impact of climate change and the expected accelerated sea level rise in the Adriatic Sea.

2. Geomorphological and Geological Settings of the Study Area

Prvić Island is located southeast of Krk Island as a natural extension of the southwest Krk ridge and has an NW-SE direction. It is separated from Krk Island by the Senjska Vrata strait and from the mainland by the Vinodol–Velebit Channel. The total surface of this island is 12.76 km^2 , and the total length of the coast is 23.12 km [22]. The karstic plateau is

higher than 300 m above mean sea level (M.S.L.). A few dry karstic valleys are deeply cut in the carbonate rock mass (Figure 1).

This island is composed predominantly of carbonate rocks: Upper Cretaceous limestone, dolomitic limestone, and Paleogene foraminiferal limestone [23]. Due to this, the landscape of the island is typical of bare karst. Paleogene siliciclastic rocks, i.e., flysch, consist of marl and sandstone in alternation [20]. The northeastern slopes of the island are very steep (Figure 1).

From a structural and tectonic point of view, Prvić Island belongs to the Krk–Rab tectonic unit [23] and represents the southeastern part of the Dinaric trending large Krk anticline. This anticline is a continuation of folded structures from the northwest, i.e., from the southeast part of Krk Island. It is an anticline with steep limbs (dip 40° – 80°), primarily vertical.

Geologic features and coastal relief on the southwestern coast considerably differ from other coastal parts. Very steep upper parts of the slopes are composed of carbonate rocks, while the more gently inclined lower parts are formed of flysch rock mass (Figure 1). The contact between carbonate rocks and flysch is an NW–SE trending reverse fault with the southwest verging and with a steep fault plane ($\sim 50^{\circ}$) [23], and it is covered by active talus [20].

The studied area around Cape Pipa is located in the central part of this coastal zone. Large rocky blocks form the cape and gravel beaches formed along both sides. This cape can be characterised as a tombolo according to the geomorphological classification [1]. Approximately 340 m towards SSE lies the Njivice Rock. It is the top of a much larger submerged rocky ridge. A large triangle-shaped shoal formed in flysch rocks is located between Cape Pipa and Njivice Rock. The bottom of that shoal is at a depth of less than 10 m below mean sea level (M.S.L.). The sandstone layers from flysch have a sub-vertical position; hence, sandstone layers give the impression of artificial walls on the sea floor [20] (Figure 2).

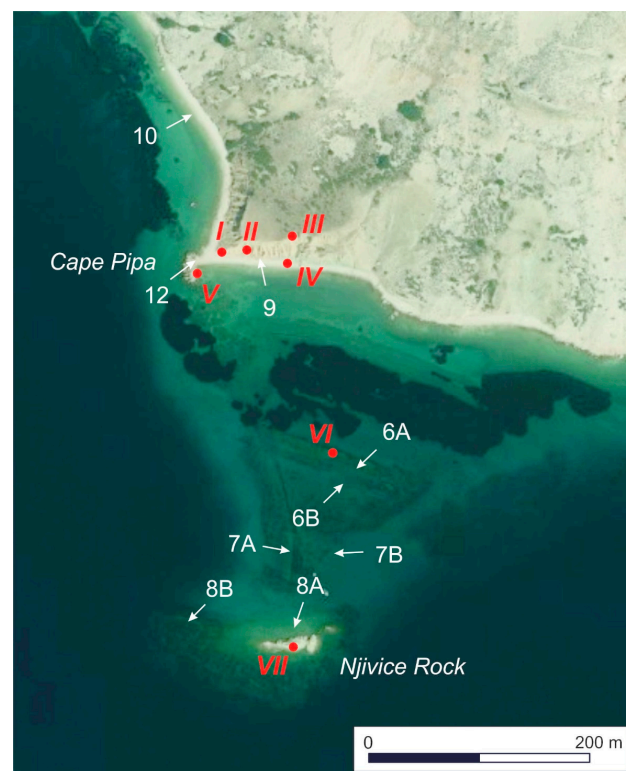


Figure 2. The ortho-photo image [24] of the investigated area with the indicated photo position being referred to further in the text (see Figures 6–12) and sample locations (Roman numbers). Dark areas are *Posidonia oceanica* meadows.

3. Methods

Field investigation and geological mapping of the studied area onshore and underwater were carried out in June and September 2022. Samples were taken during mapping. Altogether, seven samples were collected for sedimentological and mineralogical analyses to determine their lithostratigraphy (Figure 2; Supplementary Materials).

Coastal area UAV surveys were conducted in June 2022. The coastal area around Cape Pipa was recorded, and a 3D point cloud was derived from UAV images. The 3D point cloud and orthomosaic were generated in Agisoft Metashape Professional, v1.7.1 software based on Structure from Motion (SfM) with Multi-View Stereo (MVS) photogrammetry. Images were captured in JPG format using the UAV DJI Phantom 4 Professional FC6310 camera with a 20-megapixel, 100 CMOS sensor, 8.8 mm focal length. Due to the complex morphology of the investigated area, images were taken from different distances from the coastline and different camera angles according to recommendations [25]. The overlap between images was constant, with all areas covered by more than 9 overlapping images. A total of 604 images were acquired for the 0.0437 km² of complex coastline. The flight altitude was 26 m, resulting in a ground resolution of 1.05 cm/pixel. Data obtained from SfM-MVS photogrammetry were very useful in interpreting the surface part of the geological map.

The underwater areas of the study site were surveyed using scuba-diving equipment and a Remotely Operated Vehicle (ROV). Photographic images of the seabed relief were taken with an underwater camera during diving, while video recordings were made with the Blueye Pioneer observation ROV. This ROV can record videos in limited visibility due to its light-sensitive, full-high-definition camera with external light, and it can manoeuvre in challenging conditions due to its unique design and propulsion system.

The ROV was deployed and controlled from a support boat anchored near the shore in the middle of the surveyed area. The recordings began directly at the sea surface and lasted until surfacing. The ROV moved according to a predetermined dive plan, i.e., along parallel transects along the slope from the coastline of Prvić Island straight towards the open sea, from −1 m to −40 m depth.

The ROV design is such that the centre of gravity is very low, and the centre of buoyancy is very high, preventing its accidental rolling or pitching. Due to this feature, it is a much simpler and accurate way of analysing underwater slope morphology.

The grain size analysis (sieving) was performed on 3 samples (talus). Thin sections were prepared on the finer-grained breccia samples, while the coarse breccia samples were examined macroscopically. Modal analyses were performed on 4 samples, where finer-grained particles were available (matrix), and on a marl sample from flysch. The 0.09–0.125 mm size fraction was used to separate heavy and light minerals, and the mineral grains were determined using the standard method [26]. The heavy mineral fraction (HMF) was separated using bromoform (CHBr₃) at a density of 2.85 g cm^{−3}.

To analyse the morphology of the seabed, we used data from the Navionics service [27]. This web service provides nautical charts from various sources combined with Sonar Chart TM HD Bathymetry data. These data were created using Navionics proprietary systems that expand existing content with sonar data contributed by the boating community [27]. The Navionics maps were imported into ArcGIS 10.7. as raster datasets, georeferenced, and the isobaths manually vectorised. Isobaths with an equidistance of 2 m down to 50 m depth and 10 m at greater depths were used to create a map, and isobaths with an equidistance of 1 m (up to 10 m depth) and 2 m (for greater depths) were used as the basis for creating geological profiles.

The impact of waves on tombolo processes was analysed with the results of wave numerical modelling. Simple numerical simulation was performed using the Simulating Waves Nearshore (SWAN) numeric model [28]. Wave simulations were carried out for the wider water area of the Grgur Channel for northwestern and southeastern wave's directions for the 50-year return period and the mean sea level. Relevant wind strengths for numerical simulation were the following: SE: 27.4 m/s; NW: 22.2 m/s. Detailed (future) investigations of these phenomena require the measurements of local sea currents and

waves due to complex coastal morphology. During the field inspection, photo and video documentation was recorded using a photo camera and UAV, and underwater photo and video documentation were recorded using a photo camera and the ROV.

Based on the obtained morphological and laboratory results, a detailed geological map and geological cross-sections of the investigated area were prepared (Figures 3 and 5).

4. Results

4.1. Geological Setting

For details on the results regarding the sedimentological and mineralogical characteristics of the samples, please refer to the Supplementary Materials.

The steep parts of coastal slopes are composed of carbonate rocks, but the more gently inclined lower parts are composed of flysch rocks. Weathered flysch rock mass (mostly marls) is partially covered by rocky fragments and blocks originating from carbonate rocks. Cape Pipa is composed of talus breccia (Figure 3).

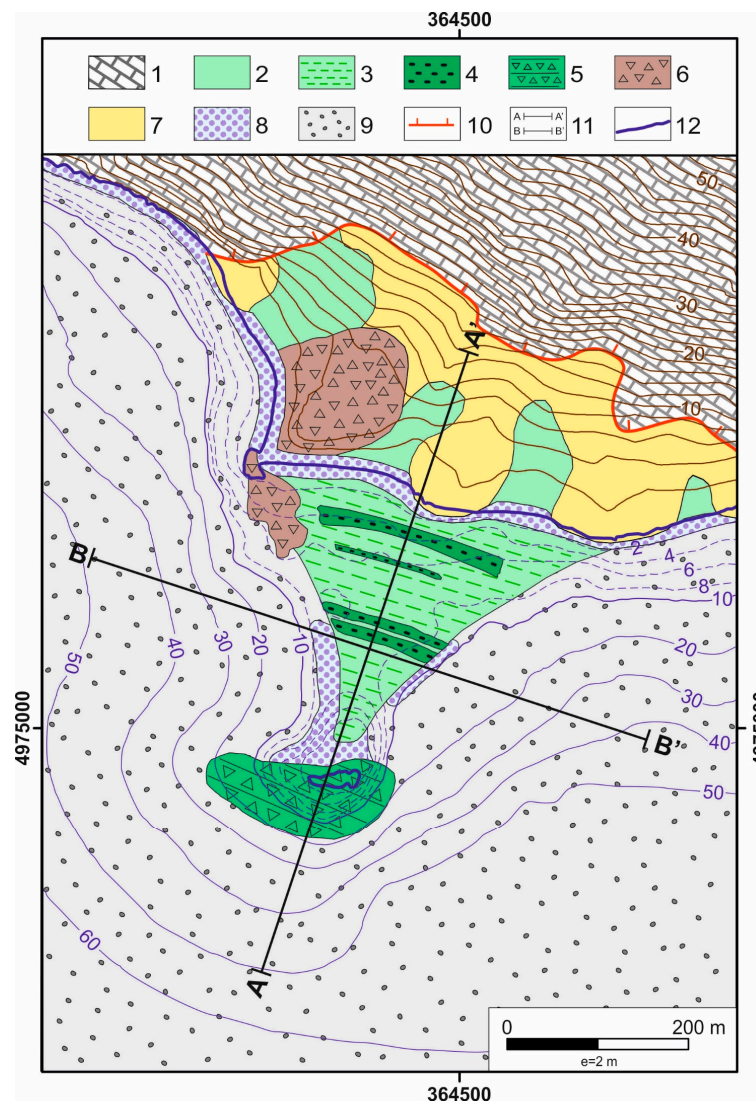


Figure 3. A simplified geological map of the investigated area: 1—carbonate rocks, 2—flysch rock (partially covered by weathered zone), 3—flysch rocks on the sea bottom, 4—vertical sandstone layers from flysch on the sea bottom, 5—carbonate breccia; 6—talus breccia, 7—active talus; 8—gravel beach; 9—muddy sand, 10—reverse fault, 11—geological cross-section (see Figure 5), 12—present-day coastline, A and B—position of cross-sections on Figure 5.

This sediment body in Cape Pipa has the form of an irregular triangle. Its height is between 10 and 12 m. The sediment body is stratified, and layers gently incline towards the northeast. Large angular fragments and blocks originating from limestones are visible in some layers. Based on the grain size analysis, this unit is poorly sorted sandy gravel, with a reddish sandy–silty matrix. The cape vertex itself is composed of collapsed blocks originating from talus breccia. Some of these blocks are located on a shoal below sea level. Blocks of talus breccia are more lithified, and thus more resistant to marine erosion. Outcrops of flysch bedrock (marls) are visible on land at the toe of the slope on the eastern side near the beach body. A narrow belt of gravel sediments extends on both sides of Cape Pipa (Figure 4).



Figure 4. The wider area of Cape Pipa (photo: D. Kalajžić): 1—limestone rock, 2—active talus, 3—flysch (marls), 4—talus breccia; 5—beach body.

Relatively narrow beach bodies stretch along both sides of the tombolo. The lower part of these bodies is located approximately 2 m below M.S.L. (Figure 4). Sub-angular to sub-rounded grains of gravel between 1 and 5 cm in diameter prevail in the beach bodies. The gravel is mostly composed of Upper Cretaceous and Palaeogene limestones, while a lower number of clasts originate from Paleogene flysch.

The Paleogene flysch (marls and sandstone in alteration) has formed a large triangular shoal between Prvić Island and Rock Njivice. The average depth of this shoal is between 5 and 7 m (Figures 2–5). The flysch sandstones (calcarenites) are vertical, and the less resistant marls are covered by coarse sand (Figures 3 and 6A,B).

Belts of rounded gravel were found on both sides of the shallow area (Figure 3). Grains originate mostly from limestone, but sandstone grains from flysch are present as well (Figure 7A,B).

The underwater slopes gently descend to a depth of 40 m on both sides and are covered by silty sand (Figures 3 and 5).

Rock Njivice is the peak of a much larger submerged phenomenon consisting of Paleogene carbonate (limestone) breccia (Figures 3 and 5). Its outcrops of this rock mass are visible on submarine slopes up to a depth of 25 m (Figure 8A,B).

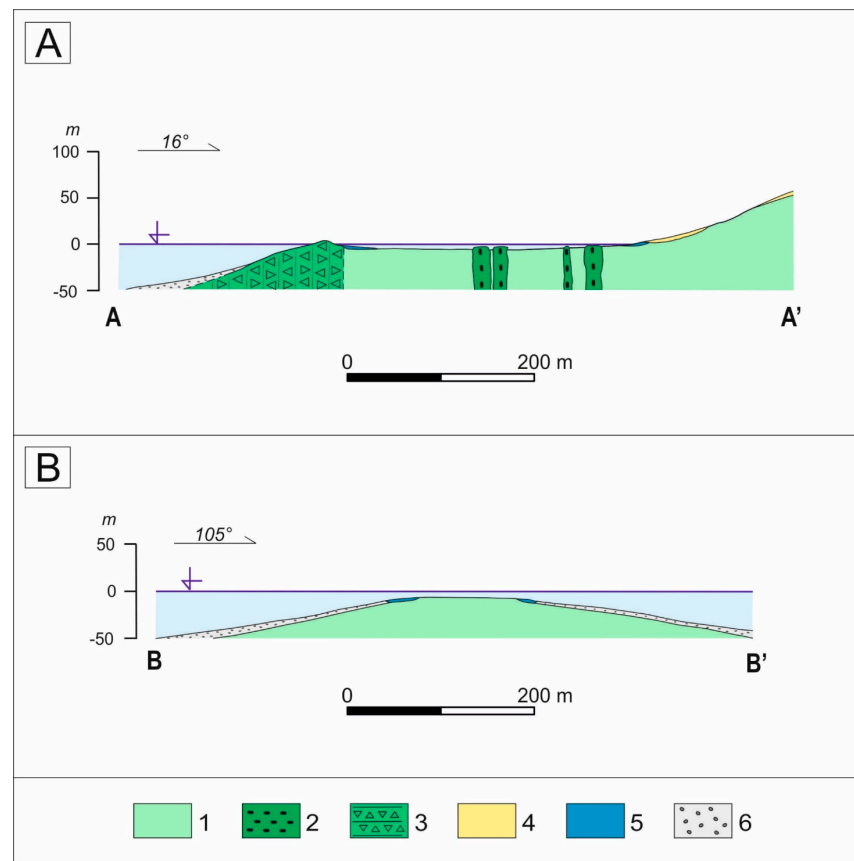


Figure 5. Geological cross-sections as indicated on Figure 3: 1—flysch-marls; 2—flysch sandstones; 3—carbonate breccia; 4—talus breccia; 5—gravel beach; 6—marine sediments. For the position of cross-sections (A,B), please see Figure 3.

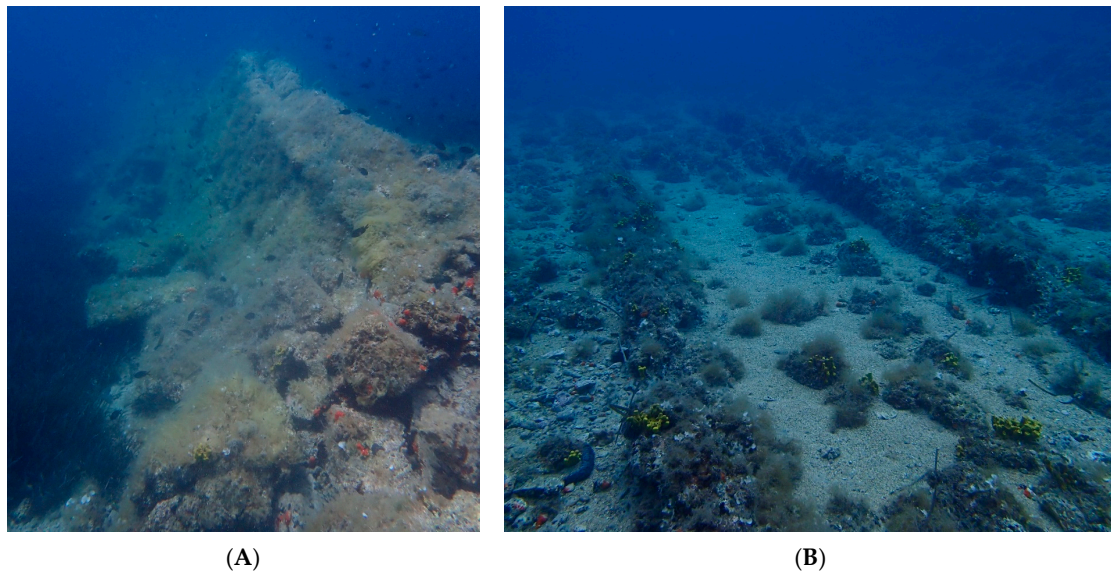


Figure 6. Details of submerged flysch elevation (A)—vertical sandstone layers, (B)—sandstone outcrops partially covered by sand (photo: Č. Benac). The position of the photos is indicated in Figure 2.



Figure 7. The remains of the submerged gravel beaches (A)—on the western side, (B)—on the eastern side (photo: Č. Benac). The position of the photos is indicated in Figure 2.



Figure 8. (A)—Rock Njivice (photo: Č. Benac), (B)—its underwater slope -25 m below M.S.L. (photo: Č. Benac). The locations of the photos are indicated in Figure 2.

4.2. Recent Geomorphological Processes

Some geomorphological processes are specific to the coastal zone and its immediate surroundings. Gravitational sediment transport and pluvial and marine erosion interact and constantly reshape the coastal zone. The average annual precipitation at Prvić Island is between 1100 and 1200 mm, but heavy precipitation with daily amounts over 100 mm/day [29] generates very intensive pluvial erosion which is visible on the triangular sediment body in Cape Pipa. Erosional channels (rills) have formed on their slopes. Due to this intensive nourishment of beach bodies is happening (Figure 9).

Pluvial erosion is not as intense on the western as on the southern slopes of Cape Pipa. The weathered flysch rock masses (mostly marl) are partially covered by active talus. Due to this, blocks and fragments constantly move down the slope and nourish beach bodies (Figure 10).



Figure 9. Erosional channels on the southern slope of Cape Pipa (photo: D. Kalajžić).



Figure 10. Outcrops of weathered flysch (greenish-grey marl) partially covered by active talus (photo: D. Kalajžić).

The Kvarner area and a part of the Grgur Channel are a semi-enclosed section of the Adriatic Sea. The waves in front of Cape Pipa are smaller compared to the open part of the Adriatic Sea due to limited fetch. The investigated coastal strip of Prvić Island is exposed to waves from the southeast (sirocco or jugo) and northwest (tramontana or tramuntana) directions [20]. The waves from the SE direction are dominant for coastal processes during storm surges, due to the combination of extreme wave heights and sea levels [30]. Figure 11 shows the results of numerical simulations for SE waves.

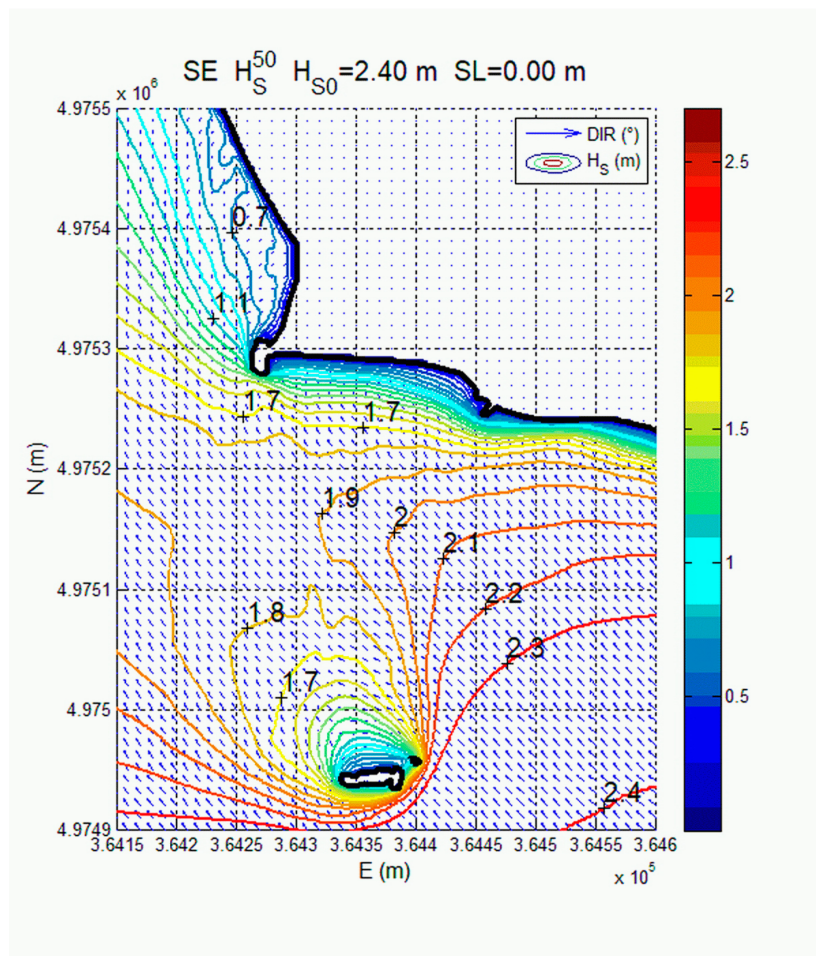


Figure 11. Numerical simulations of significant wave heights from SE wave directions for a 50-year return period.

Due to large slope of the seabed, relatively high waves reach the coast at Cape Pipa, which is why coastal processes are intense. Accumulated sediments are protected by the natural tombolo which has formed due to resistant breccia blocks. Since the waves arrive parallel to the beach due to wave refraction, sediment longshore migrations on the tombolo are not produced. The waves on the beach north of Cape Pipa do not cause beach erosion due to favourable wave heights and directions (Figure 11). Waves attacks are stronger on the southern beach during southeastern wind (jugo). Cape Pipa has a significant influence on wave diffraction and shoaling, and a wave shadow zone enables tombolo stability (Figure 12).

The sea level has continuously been measured since 1929 at the nearest tide gauge in Bakar near Rijeka city. Extremely high sea levels have been recorded: 1.18 m CVD, 1.17 m CVD on 1 December 2008, 1.22 m CVD on 1 November 2012, and 1.27 m CVD on 29 October 2018 [30]. A comparison of the georeferenced aerial images from 1968, 2011, 2014, 2018, and 2020 showed cliff recession on Cape Pipa and a decrease in beach width on the southern side [24]. Based on our observations during underwater investigations, strong currents appear on the shoal. These wind-driven currents have a direction towards the west and a speed of more than 0.5 m/s during the northeast wind (bura or bora).



Figure 12. Obstacle of blocks originating from talus breccia in front of Cape Pipa (photo: D. Kalajžić).

5. Discussion

5.1. Geomorphological Evolution

The intensity of erosion and accumulation changed in space and time, under sea level changes during geological history [31]. Sea level oscillations during the Late Pleistocene and Holocene in the Mediterranean and Adriatic seas were significant [32]. These changes in the erosion base left more pronounced traces on the flysch rocks that prevails in the Grgur Channel compared to the more resistant carbonate rocks on present-day Prvić Island and Njivice Rock. The sea level began to fall and fluctuated between -20 m and -50 m below the present M.S.L. from 110 ka to 75 ka B.P. [32]. The changes in paleogeographic conditions were already pronounced between 40 m and 50 m below M.S.L. During this period, wide marine terraces probably formed around the described shoal in the present Grgur Channel. Traces of submerged karstic valleys are located up to -40 m on the northeast coast of the Velebit Channel. Erosional disconformity is visible in the echo-sounder cross-section [33]. The sea level oscillated between -50 m and -80 m below present M.S.L. between 75 ka and 30 ka B.P. The sea retreated from a large part of the present Grgur Channel. Terrestrial conditions prevailed during this period and erosional processes of the exposed flysch rock mass were intensive. At the same time, the accumulation of slope sediments happened, and the initial form of the present Cape Pipa was probably formed. It is possible that the body of talus breccia was formed in the earlier part of the Pleistocene due to a higher degree of lithification. Complete marine regression occurred in the Kvarner area when the sea level dropped to a depth of -100 to -120 m during the Last Glacial Maximum (LGM), and the Kvarnerić basin possibly became polje [33]. Intensive erosional and accumulation processes continued during this period.

From the end of the LGM, the sea level rose in the Mediterranean Sea [32]. The sea level slowed around 7000 years ago in the Adriatic Sea [34–36]. The conditions for forming this submerged shoal came about during this slow rise. However, it is possible that the shoal is

much older, e.g., it was formed in the Pleistocene and was reworked during the Holocene. A very slow process of bioerosion prevails in carbonate rocks. Mechanical erosion is more highly expressed in the less resistant flysch rocks and Quaternary deposits [37]. The underwater elevation around Njivice Rock provides an obstacle to waves in the shallow zone (Figure 13).

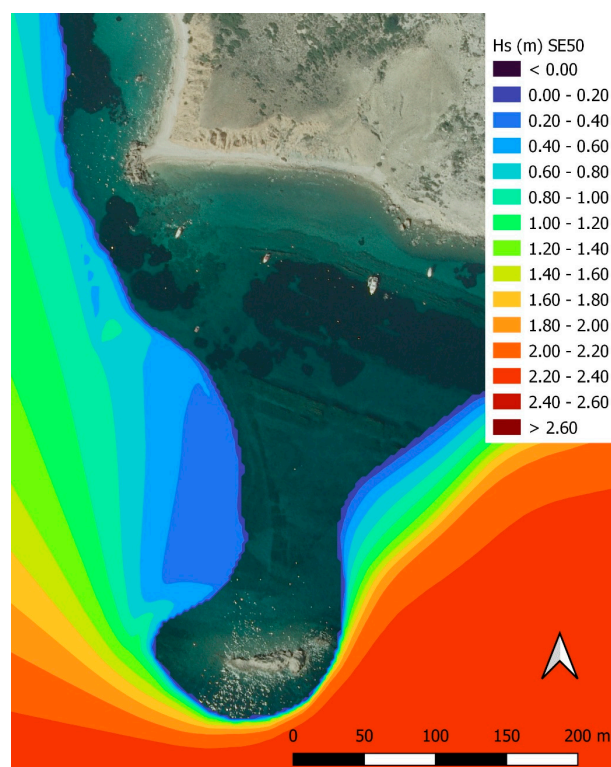


Figure 13. Significant wave heights H_s from SE waves during sea level -8 m below present M.S.L.

Conditions for forming gravel beach bodies were created during the slow sea-level rise. Wave attacks were weaker on the western side of the tombolo (wave shadow or protected zone) during the slow sea level rise, so a larger body of the former beach is visible there compared to the eastern part (Figure 3). The sea probably flooded the shallow zone at the beginning of the relative sea level stagnation in the Holocene. The vertical position of the more resistant sandstone layers of flysch helped to protect against marine erosion. A significant proportion of the body of talus breccia was eroded around Cape Pipa. Collapsed blocks provided an obstacle to waves and played an important role in the formation of the tombolo (Figures 3 and 12).

5.2. Prediction Geomorphological Changes in the Future

Sea level rise in the range of 2.0 ± 0.9 and 3.4 ± 1.1 mm/yr. has been detected from the beginning of instrumental measurements in the Adriatic Sea [38]. According to new analyses, the predicted sea level rise could be 19–33 cm (2046–2065) and 32–65 cm (2081–2100) [39]. New climate models predict extreme storm waves [40] and increased marine erosion in the North Adriatic Sea [41].

Long-term investigations have shown that beach erosion is increasing even on the relatively sheltered coast of the Mediterranean Sea [42]. Beach erosion can take the form of a long-term and irreversible geomorphological phenomenon caused by sea level rises and short-term erosion caused by storm surges and waves, which may or may not result in permanent shoreline retreats but can, nevertheless, be devastating [43].

The current environment appears to have generated an equilibrium, with sediment supply raising the level of the tombolo on Cape Pipa as sea level has risen in the recent

past. So, with future rises in sea level, this balance could continue, and this tombolo could remain in a similar position. Alternatively, a faster rate of rise in sea level could drown the feature or increase the rate of erosion.

However, it is questionable whether marine erosion or wave attacks in combination with increased slope erosion can improve beach nourishment and thus reduce the negative effect of sea level rises.

The beach body will not be flooded during a high tide of +0.60 m above the present M.S.L. (Figure 14A). The dissipation of wave energy takes place on it, and erosion does not occur. More likely, the accumulation of sediments occurs. However, the waves reach the foot of the slope, increasing the erosion, and the beach body is completely flooded during an extremely high tide of +1.20 m above present M.S.L. The waves diffract around the cape vortex and submerged beach; because of this, there is no major erosion (Figure 14B). In the case of a predicted sea level rise of 60 cm, during an extremely high tide of 1.80 m above the present M.S.L., the function of the cape vortex for wave protection is reduced, and if there is no increased sediment supply, permanent erosion will likely occur. Sea level rises and storms can intensify the cliff erosion and thus sediment supply, which could cause a system of equilibrium (Figure 15).

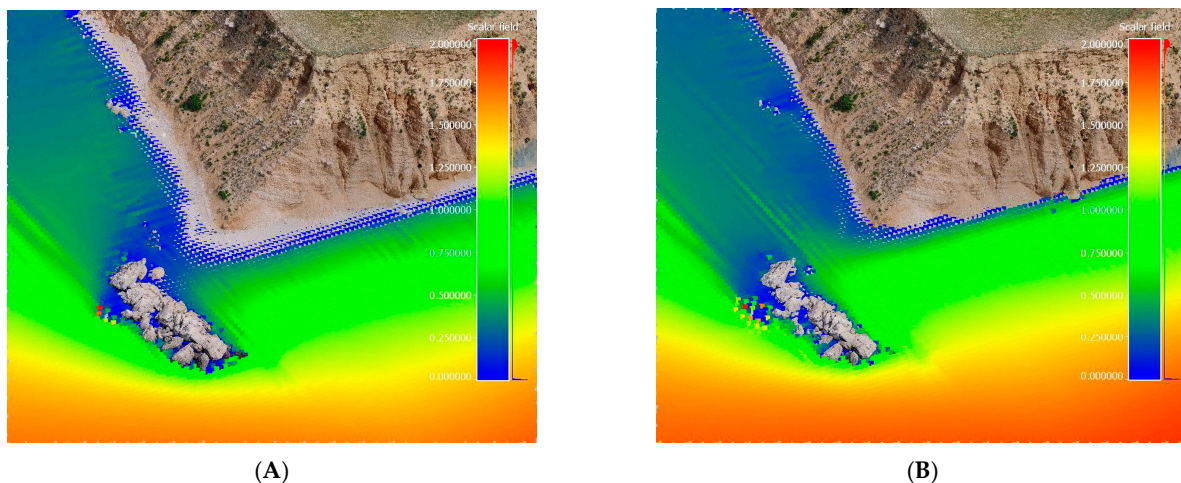


Figure 14. (A) Significant wave heights H_s at +0.60 m above present M.S.L. (B) Significant wave heights H_s at +1.20 m above present M.S.L.

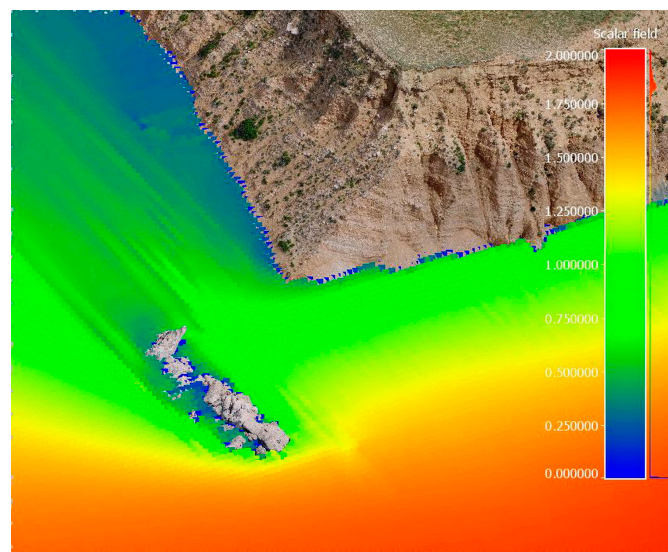


Figure 15. Significant wave heights H_s at +1.80 m above present M.S.L.

This studied area is formally part of the NATURA 2000 network [21]. However, there is no effective protection from human activities, although the coast and the seabed are exposed to strong ecological pressure during the tourist season. This especially applies to *Posidonia oceanica* meadows, which are located on the northwestern margin of their habitat in the Kvarner area (Figure 2). *Posidonia oceanica* meadows are one of the priority habitats of the European Union's Habitats Directive [44].

6. Conclusions

The recent tombolo and the much bigger submerged tombolo are located on the southwestern coast of Prvić Island between Cape Pipa and Njivice Rock. The inland part of the recent tombolo has the form of an irregular triangle and consists of talus breccia. Large collapsed rocky blocks from the talus breccia formed the cape vertex, and gravel beaches are located along both sides of this body. A large triangular shoal consists of flysch rock. Parallel outcrops of vertical sandstone layers look like artificially built walls and are more than a hundred metres long. Submarine slopes gently descend to a depth of 40 m on both sides and are covered by silty sand. Rock Njivice consists of carbonate breccia located on the top of this elevation.

The conditions for forming triangular shoal-like tombolos occurred during the slow sea level rise in the Adriatic Sea in the Holocene. The submerged ridge around the present Njivice Rock had the role of an obstacle to waves in the shallow and flattened area. However, it is possible that the shoal is much older, e.g., it was formed in the Pleistocene and was reworked during the Holocene.

Cape Pipa is in a state of equilibrium in the present climatic and oceanographic conditions. The wave direction and energy behind this cape are favourable for sediment accumulation and retention due to reduced erosion caused by longshore currents. Planar and rill erosion is intensive on slopes of talus breccia, and georeferenced aerial images from different periods showed a small cliff recession. So, with future rises in sea level, this balance could continue, and this tombolo could remain in a similar position. Alternatively, the faster rate of sea level rise could drown the feature or increase the rate of erosion.

The recent tombolo and the much bigger submerged tombolo shapes are unique phenomena along the Croatian coast of the Adriatic Sea. They represent formations of exceptional geoscientific value, formed in the unique changing conditions of the coastal environment, and their formal protection, further research, and high-quality interpretation are needed.

Supplementary Materials: The following supporting information can be downloaded at: <https://www.mdpi.com/article/10.3390/jmse12091575/s1>.

Author Contributions: Conceptualisation, Č.B. and N.B.; field investigations, Č.B. and L.M.; sedimentological analysis, L.W.; numerical simulation of waves, I.R.; preparation of figures, N.B., Č.B. and I.R.; writing—review and editing, Č.B., N.B., L.W., L.M. and I.R. All authors have read and agreed to the published version of the manuscript.

Funding: This research has been partially financed by the University of Rijeka (Uniri-zip-2103-6-22). Sedimentological analyses were performed at the Croatian Geological Survey as part of the GORIK (Geological evolution of synorogenic and post-orogenic sedimentary systems of the islands of Rab and Krk) project financed by NextGenerationEU.

Institutional Review Board Statement: Not applicable.

Informed Consent Statement: Not applicable.

Data Availability Statement: The original contributions presented in the study are included in the article/Supplementary Material, further inquiries can be directed to the authors.

Acknowledgments: The authors thank their colleague, Ladislav Fuček, for their useful advice while preparing this article. The authors also thank their colleague, Duje Kalajžić, for excellent photos taken using the UAV technique and for help with terrain analysis using SfM-MVS photogrammetry.

Conflicts of Interest: The authors declare no conflicts of interest.

References

1. Ward, S. Tombolo. In *Encyclopedia of Geomorphology*; Goudie, A.S., Ed.; Routledge: London, UK; IAG: Christchurch, New Zealand, 2004; p. 1054.
2. Marriner, N.; Goiran, J.P.; Morhange, C. Alexander the Great's Tombolos at Tyre and Alexandria, Eastern Mediterranean. *Geomorphology* **2008**, *100*, 377–400. [[CrossRef](#)]
3. Gosseaume, E. Le Tombolo Triple d'Orbetello (Toscane). *Bull. Soc. Languedoc Geogr.* **1973**, *7*, 3–11.
4. Ceylan, M. General Overview of the Tombolos on Turkey's Coastlines. *World Appl. Sci. J.* **2012**, *16*, 907–914.
5. Davies, J.L. *Geographical Variation in Coastal Development*; Longman: London, UK, 1980.
6. Schwartz, M.L.; Granö, O.; Pyökäri, M. Spits and Tombolos in the Southwest Archipelago of Finland. *J. Coast. Res.* **1989**, *5*, 443–451.
7. Sanderson, P.G.; Eliot, I.G. Shoreline Salients, Cuspate Forelands and Tombolos on the Coast of Western Australia. *J. Coast. Res.* **1996**, *12*, 761–773.
8. Kan, H.; Hori, N.; Kawana, T.; Kaigara, T.; Ichikawa, K. The Evolution of a Holocene Fringing Reef and Island: Reefal Environmental Sequence and Sea Level Change in Tonaki Island, the Central Ryukyus. *Atoll Res. Bull.* **1997**, *443*, 1–20. [[CrossRef](#)]
9. Flinn, D. The Role of Wave Diffraction in the Formation of St. Ninian's Ayre (Tombolo) in Shetland, Scotland. *J. Coast. Res.* **1997**, *13*, 202–208.
10. Hansom, J.D. St Ninian's Tombolo, Shetland. In *Coastal Geomorphology of Great Britain. Geological Conservation Review Series No. 28*; May, V.J., Hansom, J.D., Eds.; Joint Nature Conservation Committee: Peterborough, UK, 2003; pp. 458–462.
11. Aiello, G.B.; De Pippo, T.; Donadio, C.; Petrosino, C. Geomorphological Evolution of Phlegrean Volcanic Islands near Naples, Southern Italy. *Z. für Geomorphol.* **2007**, *51*, 165–190. [[CrossRef](#)]
12. Vu, M.T.; Lacroix, Y.; Nguyen, V.T. Empirical Equilibrium Beach Profiles Along the Eastern Tombolo of Giens. *J. Mar. Sci. Appl.* **2018**, *17*, 241–253. [[CrossRef](#)]
13. Vu, M.T.; Lacroix, Y.; Nguyen, V.T. Investigating the Effects of Sea-Level Rise on Morphodynamics in the Western Giens Tombolo, France. *IOP Conf. Ser. Earth Environ. Sci.* **2018**, *167*, 012027. [[CrossRef](#)]
14. Marriner, N.; Morhange, C.; Meulé, S. Holocene Morphogenesis of Alexander the Great's Isthmus at Tyre in Lebanon. *Proc. Natl. Acad. Sci. USA* **2007**, *104*, 9218–9223. [[CrossRef](#)] [[PubMed](#)]
15. Torab, M. Geomorphological & Geoarchaeological Indicators of the Holocene Sea-Level Changes on Ras El Hekma Area, NW Coast of Egypt. *J. Afr. Earth Sci.* **2016**, *114*, 85–95. [[CrossRef](#)]
16. Pikelj, K.; Juračić, M. Eastern Adriatic Coast (EAC): Geomorphology and Coastal Vulnerability of a Karstic Coast. *J. Coast. Res.* **2013**, *29*, 944–957. [[CrossRef](#)]
17. HGI. *Geološka Karta Republike Hrvatske 1:300.000*; Hrvatski geološki Institute: Zagreb, Croatia, 2009.
18. Benac, Č.; Juračić, M. Geomorphological Indicators of the Sea Level Changes during Upper Pleistocene (Würm) and Holocene in the Kvarner Region. *Acta Geogr. Croat.* **1998**, *33*, 27–45.
19. Juračić, M.; Benac, Č.; Crmarić, R. Seabeded and Surface Sediments Map of the Kvarner Bay, Adriatic Sea, Croatia. *Geol. Croat.* **1999**, *52*, 131–140.
20. Benac, Č.; Bočić, N.; Ružić, I. On the Origin of Both a Recent and Submerged Tombolo on Prvić Island in the Kvarner Area (Adriatic Sea, Croatia). *Geol. Croat.* **2019**, *72*, 195–203. [[CrossRef](#)]
21. Institute for Environmental and Nature Protection of the Ministry of Economy and Sustainable Development Biportal. Available online: <https://biportal.hr/gis/> (accessed on 3 May 2024).
22. Duplančić Leder, T.; Ujević, T.; Čala, M. Coastline Lengths and Areas of Islands in the Croatian Part of the Adriatic Sea Determined from the Topographic Maps at the Scale of 1:25,000. *Geoadria* **2004**, *9*, 5–32. [[CrossRef](#)]
23. Mamužić, P.; Milan, A.; Korolija, B.; Borović, I.; Majcen, Ž. *Basic Geological Map of SFRY 1:100,000, Rab Sheet*; Croatian Geological Survey: Beograd, Serbia, 1969.
24. GEOPORTAL State Geodetic Administration Geoportalsystem. Available online: <https://geoportalsystem.dgu.hr/> (accessed on 19 February 2024).
25. James, M.R.; Robson, S. Straightforward Reconstruction of 3D Surfaces and Topography with a Camera: Accuracy and Geoscience Application. *J. Geophys. Res. Earth Surf.* **2012**, *117*, 03017. [[CrossRef](#)]
26. Mange, M.A.; Maurer, H.F.W. *Heavy Minerals in Colour*; Chapman and Hall: London, UK, 1992. [[CrossRef](#)]
27. NAVIONICS Navionics Chart Viewer. Available online: <https://webapp.navionics.com> (accessed on 17 January 2024).
28. Booiij, N.; Ris, R.C.; Holthuijsen, L.H. A Third-Generation Wave Model for Coastal Regions 1. Model Description and Validation. *J. Geophys. Res. Ocean.* **1999**, *104*, 7649–7666. [[CrossRef](#)]
29. Zaninović, K.; Gajić-Čapka, M.; Perčec Tadić, M.; Vučetić, M.; Milković, J.; Bajić, A.; Cindric Kalin, K.; Cvitan, L.; Katušin, Z.; Kaučić, D.; et al. *Climate Atlas of Croatia 1961–1990, 1971–2000*; Zaninović, K., Ed.; Meteorological and Hydrological Service: Zagreb, Croatia, 2008.
30. Ružić, I.; Benac, Č.; Dugonjić Jovančević, S.; Radišić, M. The Application of UAV for the Analysis of Geological Hazard in Krk Island, Croatia, Mediterranean Sea. *Remote Sens.* **2021**, *13*, 1790. [[CrossRef](#)]

31. Cowell, P.J.; Thom, B.G. Morphodynamics of Coastal Evolution. In *Coastal Evolution*; Carter, R.W.G., Woodroffe, C.D., Eds.; Cambridge University Press: Cambridge, UK, 1997; pp. 33–86.
32. Benjamin, J.; Rovere, A.; Fontana, A.; Furlani, S.; Vacchi, M.; Inglis, R.H.; Galili, E.; Antonioli, F.; Sivan, D.; Miko, S.; et al. Late Quaternary Sea-Level Changes and Early Human Societies in the Central and Eastern Mediterranean Basin: An Interdisciplinary Review. *Quat. Int.* **2017**, *449*, 29–57. [[CrossRef](#)]
33. Benac, Č.; Bočić, N.; Juračić, M. Geomorphologic Changes of the Velebit Channel during Late Pleistocene and Holocene (NE Adriatic). *Geogr. Fis. e Din. Quat.* **2022**, *45*, 41–54. [[CrossRef](#)]
34. Pirazzoli, P.A. A Review of Possible Eustatic, Isostatic and Tectonic Contributions in Eight Late-Holocene Relative Sea-Level Histories from the Mediterranean Area. *Quat. Sci. Rev.* **2005**, *24*, 1989–2001. [[CrossRef](#)]
35. Lambeck, K.; Antonioli, F.; Purcell, A.; Silenzi, S. Sea-Level Change along the Italian Coast for the Past 10,000 Yr. *Quat. Sci. Rev.* **2004**, *23*, 1567–1598. [[CrossRef](#)]
36. Surić, M. Reconstructing Sea-Level Changes on the Eastern Adriatic Sea (Croatia)—An Overview. *Geoadria* **2009**, *14*, 181–199. [[CrossRef](#)]
37. Juračić, M.; Benac, Č.; Pikelj, K.; Ilić, S. Comparison of the Vulnerability of Limestone (Karst) and Siliciclastic Coasts (Example from the Kvarner Area, NE Adriatic, Croatia). *Geomorphology* **2009**, *107*, 90–99. [[CrossRef](#)]
38. Tsimplis, M.; Raicich, F.; Fenoglio, L.; Shaw, A.; Marcos, M.; Somot, S.; Bergamasco, A. Recent Developments in Understanding Sea Level Rise at the Adriatic Coasts. *Phys. Chem. Earth Parts A/B/C* **2009**, *40–41*, 59–71. [[CrossRef](#)]
39. Republic of Croatia. *Climate Change Adaptation Strategy in the Republic of Croatia for the Period until 2040 with a View to 2070*; Croatian Parliament: Zagreb, Croatia, 2020.
40. Bonaldo, D.; Bucchignani, E.; Ricchi, A.; Carniel, S. Wind Storminess in the Adriatic Sea in a Climate Change Scenario. *Acta Adriat.* **2017**, *58*, 195–208. [[CrossRef](#)]
41. Gallina, V.; Torresan, S.; Zabeo, A.; Rizzi, J.; Carniel, S.; Sclavo, M.; Pizzol, L.; Marcomini, A.; Critto, A. Assessment of Climate Change Impacts in the North Adriatic Coastal Area. Part II: Consequences for Coastal Erosion Impacts at the Regional Scale. *Water* **2019**, *11*, 1300. [[CrossRef](#)]
42. Andreadis, O.; Chatzipavlis, A.; Hasiotis, T.; Monioudi, I.; Manoutsoglou, E.; Velegrakis, A. Assessment of and Adaptation to Beach Erosion in Islands: An Integrated Approach. *J. Mar. Sci. Eng.* **2021**, *9*, 859. [[CrossRef](#)]
43. Nicholls, R.J.; Cazenave, A. Sea-Level Rise and Its Impact on Coastal Zones. *Science* **2010**, *328*, 1517–1520. [[CrossRef](#)] [[PubMed](#)]
44. European Commission. Council Directive 92/43/EEC of 21 May 1992 on the Conservation of Natural Habitats and of Wild Fauna and Flora. *Off. J. Eur. Union* **1992**, *206*, 7–50.

Disclaimer/Publisher’s Note: The statements, opinions and data contained in all publications are solely those of the individual author(s) and contributor(s) and not of MDPI and/or the editor(s). MDPI and/or the editor(s) disclaim responsibility for any injury to people or property resulting from any ideas, methods, instructions or products referred to in the content.